Hindawi
Advances in Materials Science and Engineering
Volume 2019, Article ID 6937540, 10 pages
https://doi.org/10.1155/2019/6937540

Research Article

Experimental Study on Long-Term Ring Deflection of Glass Fiber-Reinforced Polymer Mortar Pipe

Sun-Hee Kim,[1] **Soon-Jong Yoon**,[2] **and Wonchang Choi**[3]

[1]*Assistant Professor, Department of Architectural Engineering, Gachon University, Seongnam, Gyeonggi-do 13120, Republic of Korea*
[2]*Professor, Department of Civil Engineering, Hongik University, Seoul 04066, Republic of Korea*
[3]*Associate Professor, Department of Architectural Engineering, Gachon University, Seongnam, Gyeonggi-do 13120, Republic of Korea*

Correspondence should be addressed to Wonchang Choi; wonchang.choi@gmail.com

Received 24 October 2018; Revised 10 January 2019; Accepted 5 February 2019; Published 3 March 2019

Guest Editor: Rishi Gupta

Long-term pressurizing of buried glass fiber-reinforced polymer (GFRP) pipe will result in the reduction of stiffness in the pipes. It leads to excessive deflections in long-term design limits. In situ tests were performed for 664 days to measure deflections of buried GFRP pipe with a large diameter of 2,400 mm. Based on the field test results, finite element analysis was conducted to determine the pipe deflections with respect to the soil conditions and buried depth as variables. Regression analysis has been conducted to determine the long-term deflection of the GFRP pipe after 50 years of construction. The long-term deflection of the GFRP pipe was less than 5 percent suggested by the existing specifications including ASTM D5365 and AWWA M45. The comparison indicates the current specifications significantly conservative to predict long-term deflection of the buried GFRP pipe.

1. Introduction

Glass fiber-reinforced polymer (GFRP) pipe exhibits excellent resilience due to the stiffness and strength of the material compared to other types of pipes. GFRP pipes are compatible with other flexible pipes. Also, GFRP pipes are used in the construction industries due to the advantages of mechanical characteristics such as light weight, high specific strength and stiffness, and high corrosion resistance.

Furthermore, the mechanical properties of GFRP pipe, which depend on the arrangement and amount of reinforcing fibers, satisfy various conditions. GFRP pipes are classified as ductile pipes because, unlike rigid pipe, they interact with the ground and resist external loads. The structural behavior of underground pipes must be considered with regard to the possible effects of the foundation, the soil surrounding the pipe, and the characteristics of the backfill.

Most studies that have investigated the durability of the pipe material have examined the long-term properties of the pipe itself. For example, Farshad and Necola [1] conducted an experimental study of the short-term and long-term behavior of GFRP pipes in underwater environments. Their study's experimental results show that the stiffness of GFRP pipes does not decrease; regression analysis predicted the GFRP pipe strength to be about 7.5 kN after 50 years.

Farshad [2] predicted the long-term behavior of multilayer pipes according to internal water pressure. Farshad estimated the long-term strength of the composite pipe by combining secondary and linear regression analysis. The analysis, design, evaluation, residual analysis, and long-term estimation of the pipe were performed via "automated design and analysis of pipes" (ADAP) software. As a result, Farshad [2] derived a new long-term estimation method to predict the long-term life of pipes composed of various layers.

Faria et al. [3] investigated the creep and relaxation behavior of glass-reinforced thermosetting polymer plastic pipes using the same reliability as conventional methods by developing a method to replace the long-term characteristics of the pipe.

Faria and Guedes [4] compared measurement errors for four types of GFRP pipes using the standard method by regression analysis of the data to reduce the prediction time long-term behavior tests of the GFRP pipe. They found the measurement error to be 10 percent less than the measurement error derived from the standard method in short-term testing.

Sargand et al. [5] investigated the behavior of thermoplastic pipes for five years when installation under at least 6.1 m to 12.2 m was applied to thermoplastic pipes, high-density polyethylene (HDPE) pipe, and polyvinyl chloride (PVC) pipe. Their results confirmed that both seasonal temperature differences and soil moisture conditions affect the earth pressure. Based on Sargand et al.'s [5] theoretical analysis, both the changes in soil conditions changes and effects of earth pressure were found to be significant.

Kim et al. [6] predicted the turbulent deflection of glass fiber-reinforced thermosetting polymer plastic pipe embedded in nuclear cooling water. Ten thousand hours of experimental data are required to predict pipe bending strain.

Yoon and Oh [7] predicted the 50-year long-term failure of GRP pipes from failure pressure and time to failure which was tested up to 10,000 hours through the sustained internal pressure test.

Na et al. [8] tested the long-term ring-bending strain (Sb) of the GFRP pipe using the standard method to predict the life of the pipe after 50 years. A comparison of the standard method and an optimized statistical method via GFRP pipe tests showed that the error was less than 8 percent. This work confirmed that the bending strain of the pipe after 50 years can be predicted using the proposed statistical method without performing tests that take 10,000 hours.

Lee et al. [9] measured the short-term behavior of a 2,400 mm large diameter reinforced thermosetting resin pipe for 387 days in a buried pipe field test and predicted long-term behavior for 40 to 60 years.

Most studies have focused on the durability of flexible pipe. Also, long-term behavior of the flexible pipe was predicted by short-term experimental test results. In order to predict the exact long-term ring deflection of buried pipe underground, the structure should be buried for a long time. However, limitations of such work include high costs and a large budget, and finding an appropriate test site.

In this study, a large diameter reinforced polymer mortar pipe (RPMP) reinforced with resin and mortar was embedded between the resin and fiberglass sections, and the long-term ring deflection of the GFRP pipe was measured for 664 days.

The safety of a buried underground GFRP pipe can be determined through the finite element analysis and predicted pipe ring deflections using the Iowa formula proposed by the American Water Works Association (AWWA M45). To predict long-term ring deflection, the long-term behavior of the GFRP pipe was predicted statistically using initial measurement data (pipe ring deflection data) proposed in American Society for Testing and Materials (ASTM D5365) [10].

2. Design Procedure for Buried GFRP Pipe

2.1. Fabrication of GFRP Pipe. The fabrication of the GFRP pipe involves a continuous filament winding process in which several mandrels are moved to wind up reinforcing fibers at multiple locations. The axial tensile strength of the pipe is increased by arranging the reinforcing fiber in the axial direction. The GFRP pipe used in this study was fabricated from RPMP that was reinforced with resin and mortar between sections that were composed of resin and glass fiber. Table 1 presents the mechanical properties of the GFRP pipe used in this study.

2.2. Structural Behavior of Buried Flexible Pipe. The structural behavior of the pipe that is embedded underground differs according to the type of external pressure. When the external load is a static load, the vertical earth pressure that is acting on the buried pipe is determined by the load on the upper part of the pipe and the area to be loaded.

In this case, the pipe buried in the ground deforms to induce earth pressure in the horizontal direction, and the vertical earth pressure generated from the load becomes greater than the horizontal earth pressure generated by the pipe deflection.

Therefore, as shown in Figure 1, under normal loading conditions, the pipe is deformed by Δ_v in the vertical direction and deformed by Δ_h in the horizontal direction.

When a preload is applied to the upper part of the pipe without consideration of the effect of the surrounding soil on the pipe deflection, the amount of pipe deflection for each direction is calculated using the following equations [11]:

$$\Delta_v = 0.149 \frac{r^3}{EI} w, \tag{1}$$

$$\Delta_h = 0.137 \frac{r^3}{EI} w, \tag{2}$$

where Δ_v is the vertical deflection (mm), Δ_h is the horizontal deflection (mm), r is the mean radius of the pipe (mm), E is the modulus of elasticity for hoop direction (MPa), I is the moment of inertia of the pipe (mm^4/mm), and w is the line load applied on top of the soil (kN/m).

Although equations (1) and (2) will differ somewhat depending on the materials that constitute the pipe, a small deflection theory is adopted. The predictions are relatively accurate within about 3 percent of pipe strain, but the accuracy is diminished slightly due to material and geometric nonlinearities above 3 percent of the pipe strain [11].

In addition, pipe stiffness (PS) must be determined in order to predict the deflection of buried pipes. The PS can be determined using equations (3a) or (3b). The PS is determined from the original stiffness test and is the value obtained by dividing the force (F) per unit length that corresponds to the 5 percent pipe strain caused by vertical displacement. The PS can be computed by the ring flexural modulus (E). The moment of inertia (I) of the pipe can be obtained from equation (3b):

Table 1: Mechanical properties of the GFRP pipe.

Material properties		GFRP pipe	Standard
	Diameter (mm)	2,400	—
	Thickness (mm)	44.5	—
Hoop	Tensile strength (MPa)	146	ASTM D2290-08 [12]
	Tensile elasticity modulus (GPa)	16.5	ASTM D2290-08 [12]
Axial	Tensile strength (MPa)	78.9	ASTM D638-10 [13]
	Tensile elasticity modulus (GPa)	9.45	ASTM D638-10 [13]
	Compressive strength (MPa)	149	ASTM D695 [14]
	Compressive modulus of elasticity (GPa)	8.97	ASTM D695 [14]
	Bending strength (MPa)	154	ASTM D790-10 [15]
	Bending modulus of elasticity (GPa)	11.5	ASTM D790-10 [15]
	Poisson's ratio	0.20	ISO 527-4 [16]

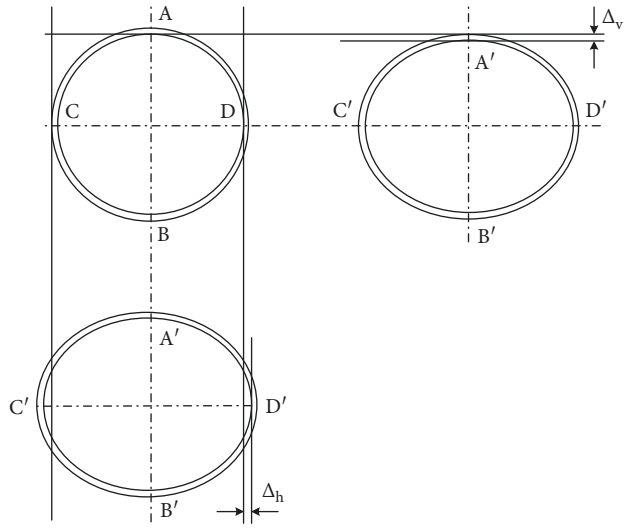

Figure 1: Ring deflection.

$$\mathrm{PS} = \frac{F}{\Delta v}, \tag{3a}$$

$$\mathrm{PS} = 6.7\frac{EI}{r^3}, \tag{3b}$$

where E is the ring flexural modulus (GPa), I is the moment of inertia of unit length ($\mathrm{mm}^4/\mathrm{mm} = -(t)^3/12$), r is the mean pipe radius ($\mathrm{mm} = (\mathrm{OD} - t)/2$), F is the force, and Δ_v is the vertical deflection (%).

The Iowa formula proposed in ASTM D2412 [17] was applied in this study to predict the deflection of the flexible buried pipe. The Iowa formula is shown in equation (4) and includes load and boundary conditions, such as the stiffness of the flexible pipe, the soil reaction force coefficient of the rebound soil, and foundation conditions for flexible underground pipes. The behavior of the flexible pipe is clearly expressed in the buried underground:

$$\Delta_h = \frac{(D_L W_c + W_L)K_X}{0.149\mathrm{PS} + 0.061E'}, \tag{4}$$

where D_L is the deflection lag factor to compensate for the time consolidation rate of the soil, dimensionless, W_c is the vertical soil load on the pipe ($\mathrm{N/m}^2$), W_L is the live load on the pipe ($\mathrm{N/m}^2$), K_X is the bending coefficient, dimensionless, PS is the pipe stiffness (kPa), E' is the composite soil constrained modulus (MPa), and Δ_h is the horizontal deflection (mm).

Equation (4) in the Iowa formula limits the deflection of the pipe to within 5 percent by applying a safety factor of 4 when pipe deflection occurs at about 20 percent. The reason for this limitation is to consider the safety of the pipe even for long-term ring deflection. The effects of pipe joint leakage also are considered [18].

3. Experimental Program

3.1. Full-Scale Field Experiments. In order to investigate the structural behavior of the GFRP pipe, the GFRP pipe composed of RPMP was buried and the soil was compacted at the underground location of the pipe. Field test was carried out at four sites of the buried GFRP pipe, as shown in Figure 2. Figure 3 shows the location of measurement for vertical and horizontal deflections of the GFRP pipe using a laser distance meter which was installed at each site.

3.2. Numerical Analysis. In order to analyze the structural behavior of the buried GFRP pipe and compare it with the field measurements, the finite-difference analysis (FDA) was carried out with respect to buried depth as variables. The MIDAS/GTS program [19] was used for two-dimensional numerical analysis. The Mohr–Coulomb failure criterion was adopted for the soil conditions which use an elasto-plastic modeling associated with a homogenous material. Linear elastic modeling was used for the beam elements for the GFRP pipe. Both end supports and bottom supports are assumed as a fixed boundary condition.

The characteristics of the pipe bedding material (PBM) are summarized in Table 2 which is obtained by field test results. Table 3 presents three cases of the compaction conditions for the GFRP pipe used for the numerical analysis in this study.

Analytical modeling takes place when 5 m, 10 m, and 16 m are filled in the upper part of the GFRP pipe, as shown in Figure 4(a). Figure 4(b) shows the grid mesh for the FDA.

Figure 5 presents displacement contour with FDA results for each case at a buried depth of 16 meter. The stress distribution surrounding the buried GFRP pipe is influenced by the characteristic of PBM. Table 4 provides a summary of the results of the FDA and experimental results. Based on the measurements, the vertical deflection and horizontal deflection were found to be the same as for the analytical results when the compaction condition of the ground around the GFRP pipe in Case 1 was well matched in the finite element

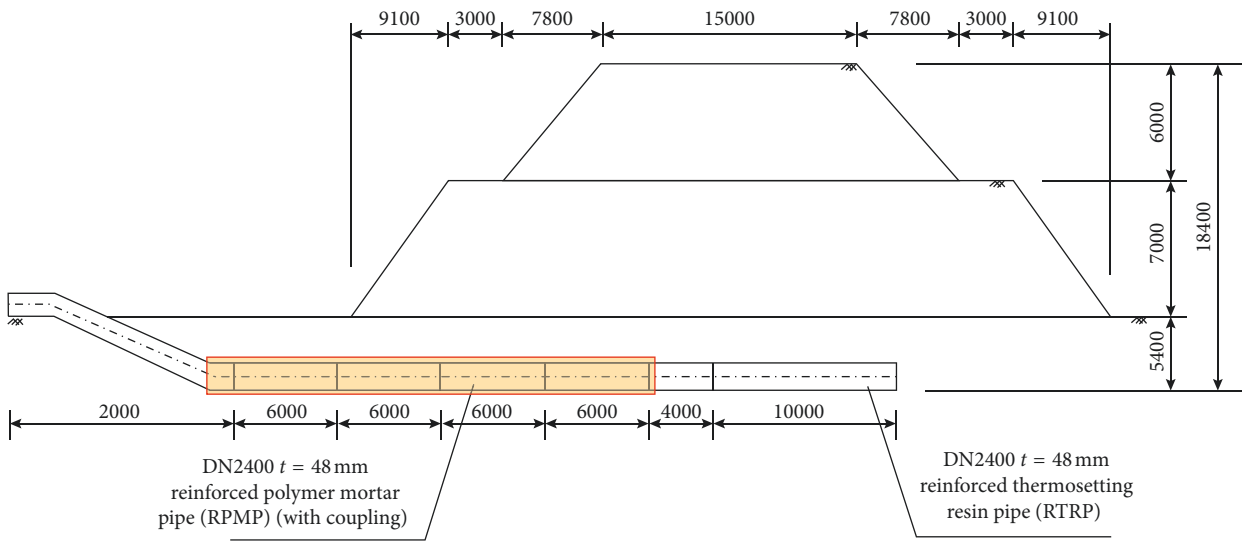

Figure 2: Side elevation of underground GFRP pipe.

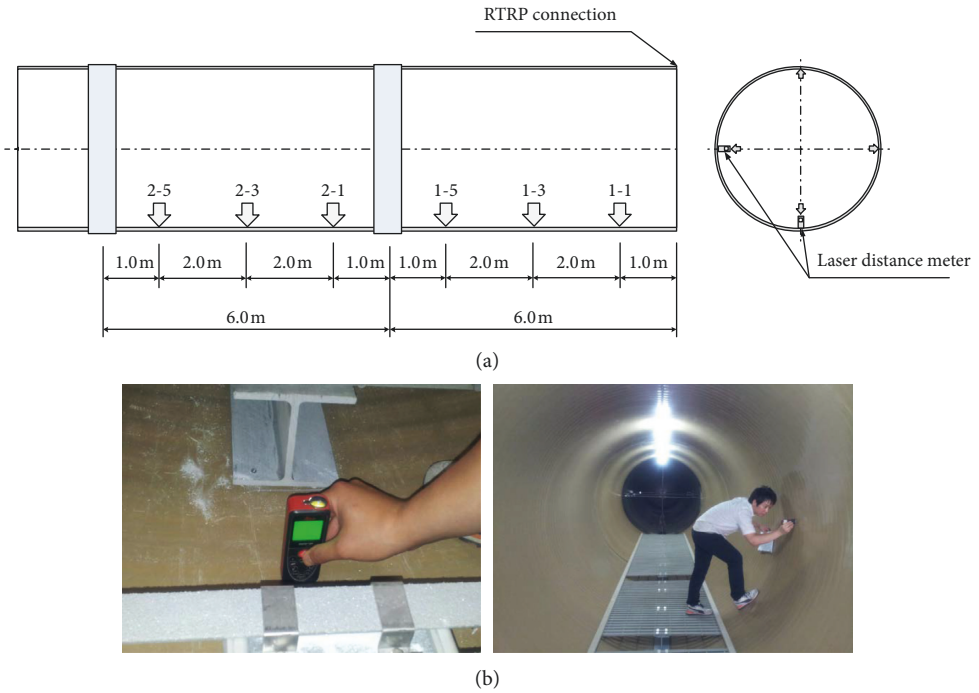

Figure 3: Measurements of GFRP pipe deflections. (a) Locations of measurement. (b) Laser distance meter and taking measurements.

Table 2: Characteristics of the soil materials [9].

Description	Soil modulus, E (kN/m^2)	Poisson's ratio, ν	Unit weight, γ_t (kN/m^3)	Viscosity, C (kN/m^2)	Internal friction angle, φ (°)
General fill	40,000	0.30	20.19	0.0	35.0
PBM #1	30,000	0.30	17.85	0.0	30.0
PBM #2	3,000	0.30	17.85	0.0	30.0
Residual soil #1	50,000	0.30	18.00	0.0	34.0
Residual soil #2	80,000	0.30	19.00	0.0	40.0
Weathered rock	15,000	0.30	20.00	30.0	35.0
Soft rock	30,000	0.25	22.00	50.0	40.0

Table 3: Soil conditions around GFRP pipe for the finite-difference analysis [9].

Description	Buried depth (m)	Soil conditions around GFRP pipe	
		Domain	Soil characteristic
Case 1	5, 10, 16	Whole of soil around GFRP pipe	PBM #1
Case 2	5, 10, 16	Center of GFRP pipe (2D) in Figure 5(a)	PBM #2
Case 3	5, 10, 16	Center of GFRP pipe (3D) in Figure 5(a)	PBM #2

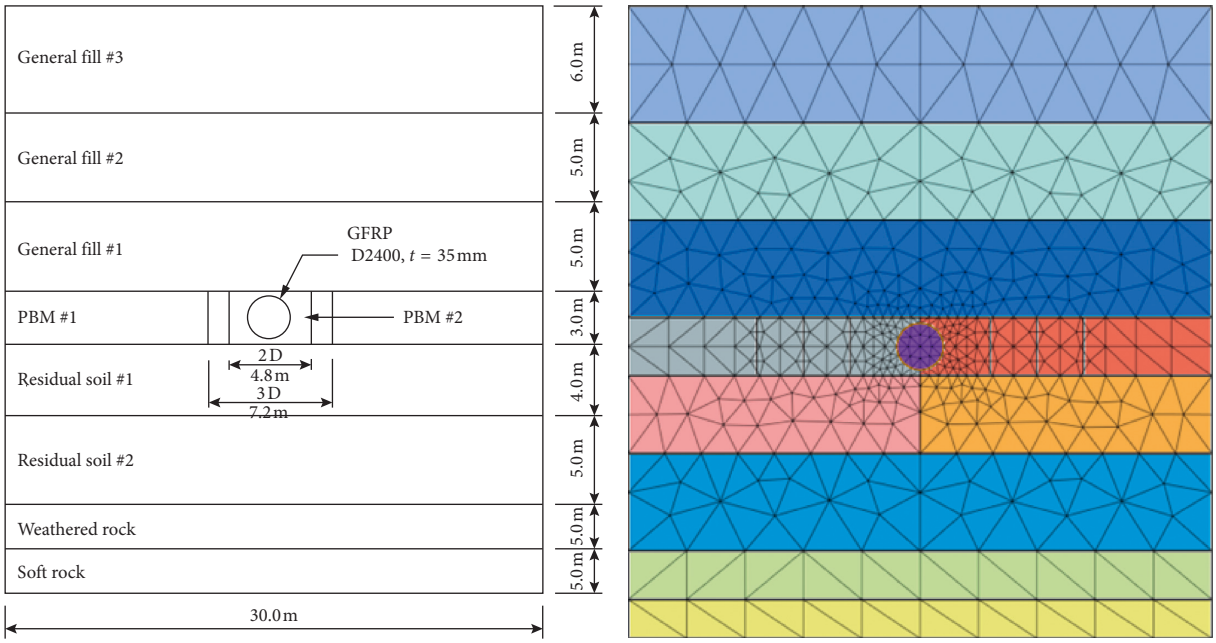

Figure 4: Finite element analysis model. (a) Schematic view. (b) Finite element analysis mesh model (2D).

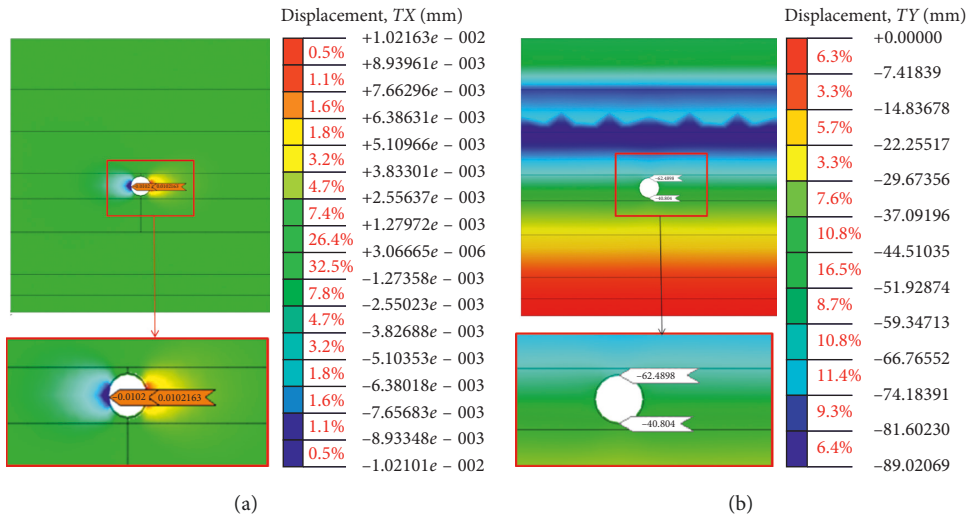

Figure 5: Continued.

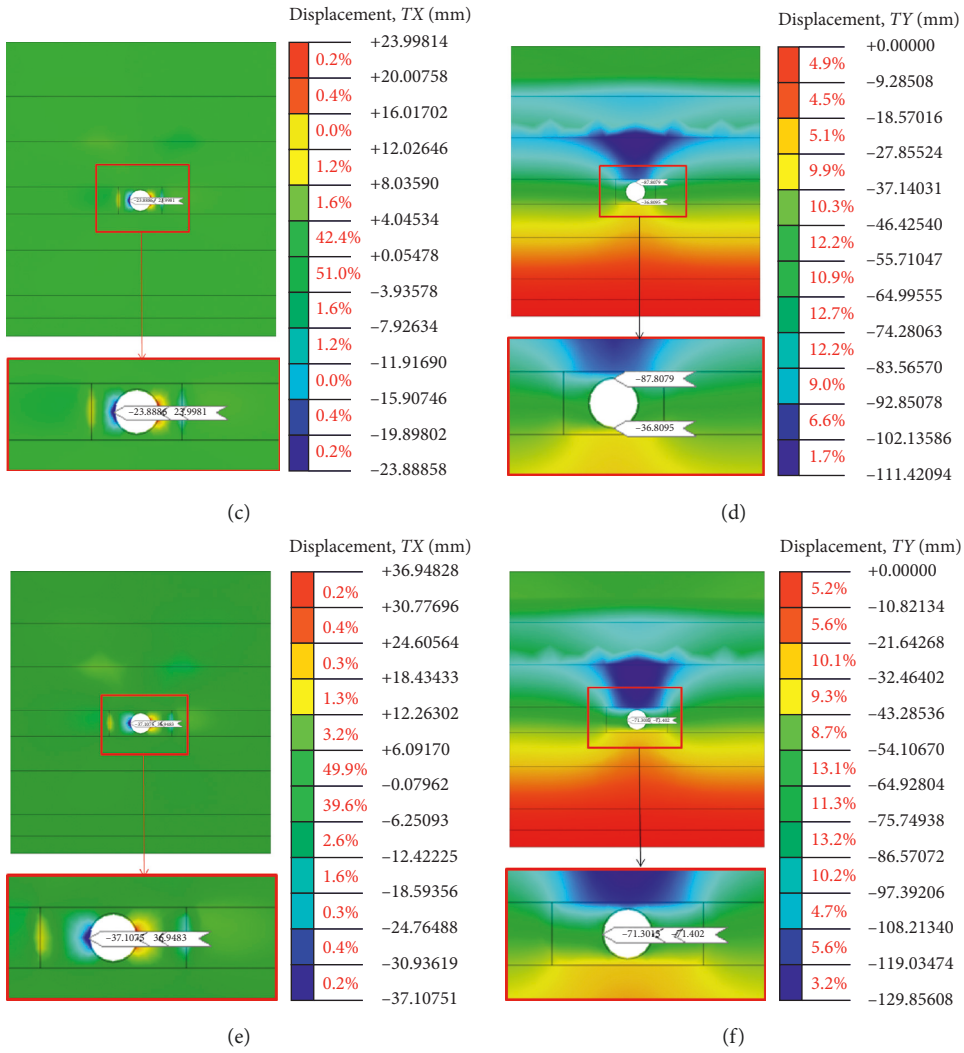

Figure 5: Finite element analysis results. (a) Horizontal deflection for Case 1 (16 m). (b) Vertical deflection for Case 1 (16 m). (c) Horizontal deflection for Case 2 (16 m). (d) Vertical deflection for Case 2 (16 m). (e) Horizontal deflection for Case 3 (16 m). (f) Vertical deflection for Case 3 (16 m).

Table 4: Comparisons of numerical analysis results and experimental results.

Buried depth (m)	Two-dimensional analytical results (%)						Experimental results (%)		AWWA M45 (%)	
	Case 1		Case 2		Case 3					
	Δ_v	Δ_h	Δ_v	Δ_h	Δ_v	Δ_h	Δ_v	Δ_h	Δ_v	Δ_h
5	−0.28	0.27	−0.75	0.71	−1.17	1.18	−0.17	0.17	−0.52	0.52
10	−0.56	0.53	−1.38	1.30	−2.06	2.07	−0.38	0.38	−1.05	1.05
16	−0.90	0.85	−2.13	2.00	−3.08	3.09	−0.71	0.54	−1.67	1.67

Note: (+): increases in diameter; (−): decreases in diameter.

analysis. The accuracy of the FDA was validated by test results, and it proved to be capable of simulating ring deflection with respect to buried condition.

The horizontal ring deflections and vertical ring deflections in Case 1 calculated by the finite-difference analysis agreed with the experimental results. According to the comparison results, it can be seen that the compaction density of soil around the buried pipe affected on the deflection of the pipe embedded underground.

4. Test Result and Discussion

4.1. Field Test Results and Prediction of Pipe Deflection. Figure 6 shows the measured vertical and horizontal displacements at 1 m, 3 m, and 5 m from the entrance of the pipe. The measured pipe deflection was within 1.5 percent. Most of the total deflection occurred within the first 30 days after construction. As soil is placed over a buried GFRP pipe, the ring tends to deflect primarily into an ellipse with a

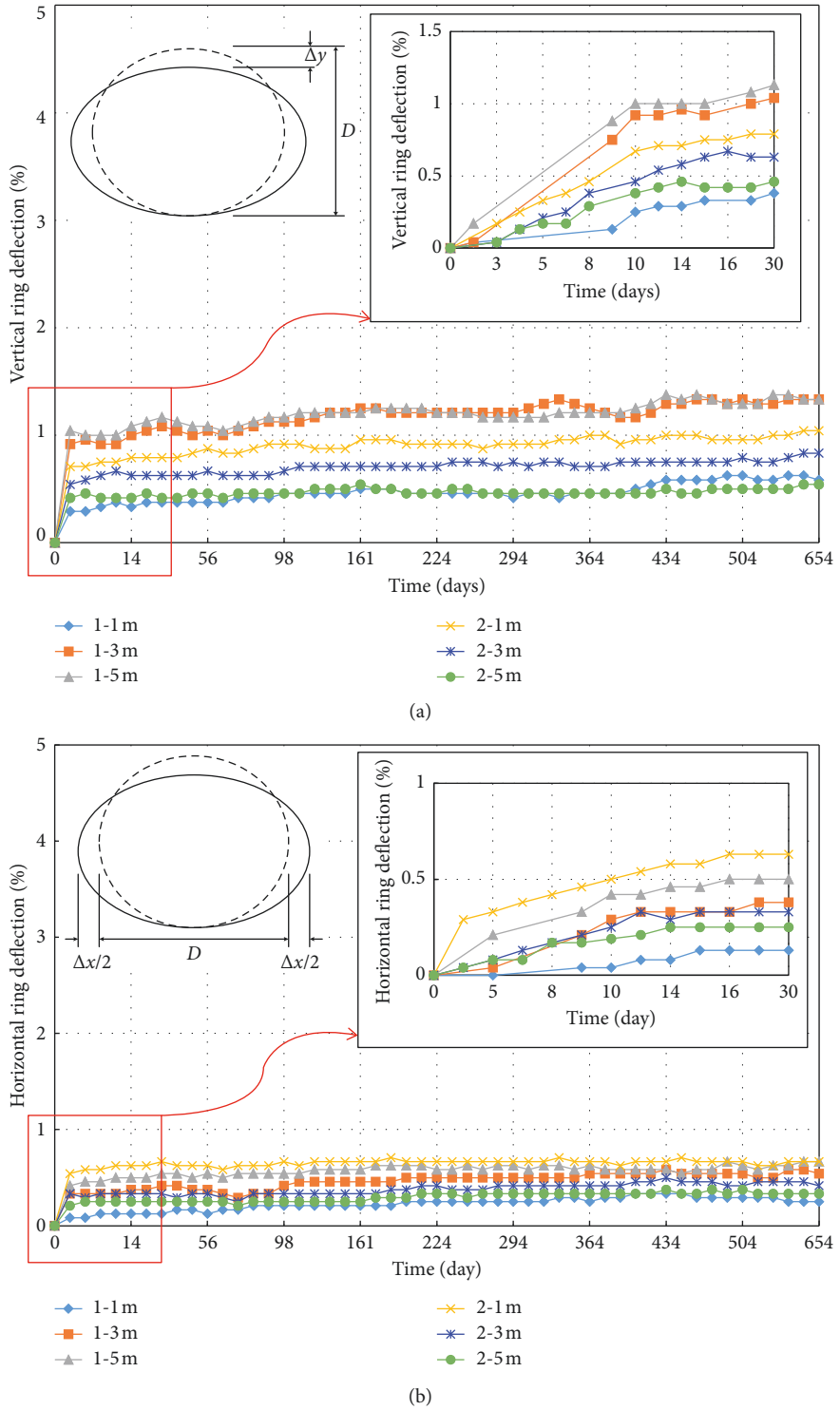

Figure 6: Measured deflections for the underground GFRP pipe.

decrease in vertical ring deflection and an almost equally increase in horizontal direction.

Figure 7 shows the comparisons between the vertical and horizontal pipe deflections and the pipe deflections in the AWWA M45 design method. The vertical pipe deflection for the case of the buried depth of 16 m is about 20 percent smaller than the pipe deflection predicted by AWWA M45. In that case, the horizontal pipe deflection was estimated to be about 10 percent smaller than the deflection predicted by AWWA M45.

The vertical pipe deflection was also about 53 percent larger than the horizontal pipe deflection. However, the difference in the maximum pipe deflection that was actually measured is about 8 mm, which is almost negligible considering the measurement error of the design parameters,

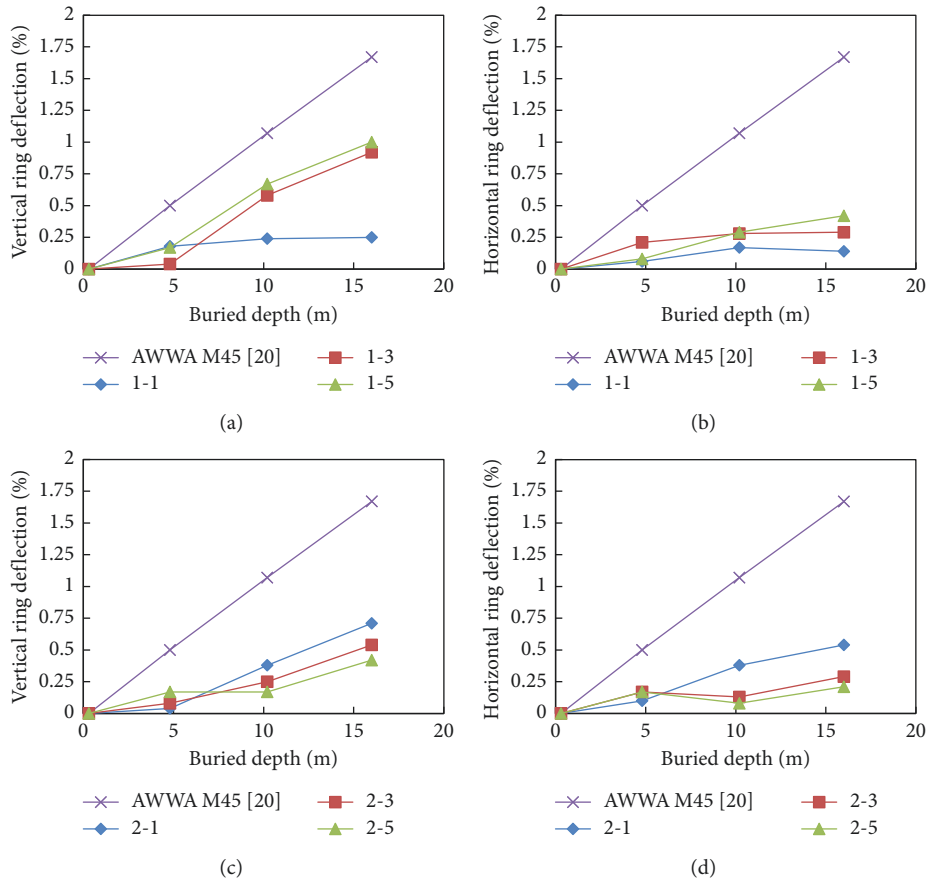

Figure 7: Comparison of ring deflection of the GFRP pipe with respect to buried depth.

such as the ground characteristics, given the 2,400 mm inner diameter of the pipe. In short, the AWWA M45 design method yields a conservative design, including the effects on long-term behavior.

The formula used in AWWA M45 for pipe deflection calculations was derived from the Iowa formula, which in turn was derived from an experimental study of small corrugated steel pipes. In the case of such small pipes, local excessive stress can be concentrated, and strict pipe deflection management is required. However, in the case of the pipe with a diameter of 2,400 mm, the curvature occurring in a pipe section is very small, and thus, the possibility of local excessive stress is negligible.

In addition, deflection occurs in the vertical direction due to the vertical load that is in turn due to the vertical deflection buried pipe, and this vertical deflection (Δ_v) is transferred to the horizontal deflection that is due to the characteristics of the circular section that is bound by the surrounding soil. Therefore, the vertical deflection is larger than the horizontal deflection ($\Delta_v > \Delta_h$) when the vertical load is not transmitted within all the horizontal deflections, but some of the energy accumulates in the pipe.

The Iowa formula is proposed to predict the horizontal deflection in this experimental study. However, in AWWA M45, the safety design (designed to produce less pipe deflection) is assumed to be the same ($\Delta_v \approx \Delta_h$) for both vertical and horizontal strains.

4.2. Effect of Pipe Stiffness in Ring Deflection. The parameters that determine the deflection of the underground GFRP pipe are the stiffness of the pipe, the stiffness of the ground, and the condition of the foundation. However, as time elapses, it is difficult to change the state of the foundation in the middle of these variables. Also, if the stiffness of the soil around the pipe is firmly consolidated, then any increase in the pipe deflection is mainly due to the mechanical properties.

In a previous study [9], the durability of the GFRP pipe did not change significantly under a low temperature range. However, the durability of the GFRP pipe may be decreased due to the various variables found in underground conditions that are used to predict pipe deflection in AWWA M45. Figure 8 shows the pipe deflection with respect to the various ring stiffness of the GFRP pipe. The pipe deflection was computed by equation (4).

The deflection of the GFRP pipe can be predicted by changing the PS from 288 kN/m^2 to zero, assuming that the GFRP pipe buried at 16 m has significantly reduced stiffness due to external environmental factors. When the PS is 288 kN/m^2, the pipe deflection is 2.515 mm, and when the PS is zero, the pipe deflection is 2.603 mm. Therefore, the effect of PS on pipe deflection is minor, having less than about 3.5 percent ring deflection. While the effect of PS and the soil foundation combined is about 96.5 percent, the fact indicates that the soil foundation is the dominant variable for pipe deflection.

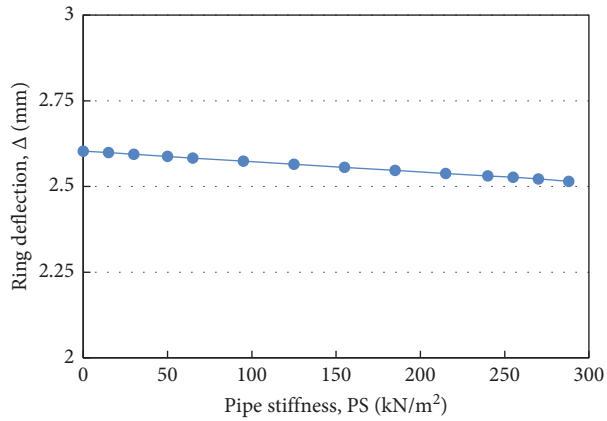

Figure 8: Ring deflection of GFRP pipe versus pipe stiffness.

Table 5: Predicted results of long-term ring deflection of pipe.

Period of time (year)	Long-term vertical deflection (%) location						Long-term horizontal deflection (%) location					
	1-1	1-3	1-5	2-1	2-3	2-5	1-1	1-3	1-5	2-1	2-3	2-5
10	0.7	1.49	1.44	1.11	0.86	0.55	0.47	0.69	0.72	0.73	0.53	0.42
20	0.77	1.57	1.5	1.17	0.9	0.56	0.55	0.76	0.75	0.75	0.57	0.45
30	0.81	1.62	1.54	1.2	0.92	0.58	0.6	0.8	0.77	0.76	0.6	0.47
40	0.84	1.66	1.56	1.22	0.94	0.58	0.65	0.83	0.79	0.77	0.62	0.49
50	0.86	1.68	1.58	1.25	0.95	0.59	0.68	0.85	0.8	0.77	0.65	0.5

4.3. Prediction of Long-Term Pipe Deflection. Although no specific method for predicting long-term pipe deflection has been developed yet, ASTM D5365 proposes a method to estimate long-term data for pipe deflection using statistical methods via the initial measurement data for pipe deflection. Equation (5) can be used to compute long-term deflection in accordance with ASTM D5365. The parameters a and b for pipe strain are defined as equations (6) and (7), respectively:

$$\text{ring deflection } (\%) = 10^{a-b\times\log_{10}t}, \tag{5}$$

where a and b are the parameters relating to ring deflection and t is the elapsed time (in hour):

$$a = Y - b \times X, \tag{6}$$

$$b = -(\gamma)^{0.5}, \tag{7}$$

where Y is the arithmetic mean of all the ring strain values, X is the arithmetic mean of all the time to failure in hours of observation, and γ is the slope of the load versus strain curve. The pipe deflection was predicted according to the time course proposed in ASTM D5365. This study predicted long-term pipe deflection up to 50 years after the GFRP pipe is buried. The computed results are summarized in Table 5.

Table 5 confirms that all of the pipe deflection that occurred after 50 years is within 5 percent. The allowable pipe deflection of 5 percent is considered to yield a very high safety factor of 4 from the structural point of view. Thus, judging from the fact that the standard of repair for pipe maintenance is limited to 7.5 percent in several of the relevant design standards, the buried GFRP pipe has sufficient structural safety and long-term durability.

5. Conclusion

In this study, pipe ring deflections were measured in the field for the buried GFRP pipe. In addition, the FDA was carried out including various parameters, such as the soil compaction density of the bedding, backfill materials, and different depths. Both the analytical and experimental results were compared and discussed.

The pipe deflection measured by the field tests indicates that the vertical load increased with an increase in the soil depth at the initial stages of construction. The increase in the pipe deflection tended to decrease with the soil depth of 16 m.

The increase in pipe deflection after the completion of the embankment appears to have been caused by the fact that the backfill stabilized over time and that some load was added to the buried pipe due to the minor settlement of the soil around the pipe.

Field tests of the buried GFRP pipes were carried out for 664 days. The measured deflection of the GFRP pipes was less than 1.5 percent during these field tests. This measured deflection of 1.5 percent was less than the 5 percent pipe deflection suggested by AWWA M45. Also, the safety of the buried GFRP pipe was verified by field tests.

Data Availability

The data sets generated during and/or analyzed during the current study are available from the corresponding author on reasonable request.

Conflicts of Interest

The authors declare that there are no conflicts of interest regarding the publication of this paper.

Acknowledgments

This work was supported by the Energy Research and Development of the Korea Institute of Energy Technology Evaluation and Planning (KETEP) grant funded by the Korea government's Ministry of Trade, Industry & Energy (no. 20161120200190). This work also supported by the Gachon University Research Fund (GCU-2018-0317).

References

[1] M. Farshad and A. Necola, "Effect of aqueous environment on the long-term behavior of glass fiber-reinforced plastic pipes," *Polymer Testing*, vol. 23, no. 2, pp. 163–167, 2004.

[2] M. Farshad, "Determination of the long-term hydrostatic strength of multilayer pipes," *Polymer Testing*, vol. 24, no. 8, pp. 1041–1048, 2005.

[3] H. Faria, A. Vieira, J. Reis, A. T. Marques, R. M. Guedes, and A. J. M. Ferreira, "Long-term behaviour of GRP pipes," *Science and Engineering of Composite Materials*, vol. 12, no. 1-2, pp. 55–62, 2005.

[4] H. Faria and R. M. Guedes, "Long-term behaviour of GFRP pipes: reducing the prediction test duration," *Polymer Testing*, vol. 29, no. 3, pp. 337–345, 2010.

[5] S. Sargand, T. Masada, B. Tarawneh, and D. Gruver, "Deeply buried thermoplastic pipe field performance over five years," *Journal of Geotechnical and Geoenvironmental Engineering*, vol. 134, no. 8, pp. 1181–1191, 2008.

[6] S.-H. Kim, J.-S. Park, and S.-J. Yoon, "Long-term ring deflection prediction of GFRP pipe in cooling water intake for the nuclear power plant," *Journal of the Korean Society for Advanced Composite Structures*, vol. 3, no. 3, pp. 1–8, 2012.

[7] S. H. Yoon and J. O. Oh, "Prediction of long term performance for GRP pipes under sustained internal pressure," *Composite Structures*, vol. 134, pp. 185–189, 2015.

[8] L. Na, Z. Sirong, C. Jianzhong, and F. Xi, "Long-term behavior of GFRP pipes: optimizing the distribution of failure points during testing," *Polymer Testing*, vol. 48, pp. 7–11, 2015.

[9] Y.-G. Lee, S.-H. Kim, J.-S. Park, J. W. Kang, and S.-J. Yoon, "Full-scale field test for buried glass-fiber reinforced plastic pipe with large diameter," *Composite Structures*, vol. 120, pp. 167–173, 2015.

[10] ASTM D5365, *Standard Test Method for Long-Term Ring-Bending Strain of "Fiberglass" (Glass-Fiber-Reinforced Thermosetting-Resin) Pipe*, ASTM, West Conshohocken, PA, USA, 2012.

[11] P. S. Bulson, *Buried Structures-Static and Dynamic Strength*, Chapman and Hall, London, UK, 1985.

[12] ASTM D2290, *Standard Test Method for Apparent Hoop Tensile Strength of Plastic or Reinforced Plastic Pipe by Split Disk Method*, ASTM, West Conshohocken, PA, USA, 2008.

[13] ASTM D638, *Standard Test Method for Tensile Properties of Plastics*, ASTM, West Conshohocken, PA, USA, 2010.

[14] ASTM D695, "Standard test method for compressive properties of rigid plastics," *Journal of Transportation Engineering*, 2010.

[15] ASTM D790, *Standard Test Method for Flexural Properties of Unreinforced and Reinforced Plastics and Electrical Materials*, ASTM, West Conshohocken, PA, USA, 2010.

[16] ISO 527-4, *Plastics-Determination of Tensile Properties-Part 4: Test Conditions for Isotropic and Orthotropic Fibre-Reinforced Plastic Composites*, ISO, Geneva, Switzerland, 1997.

[17] ASTM D2412, *Standard Test Method for Determination of External Loading Characteristics of Plastic Pipe by Parallel-Test Loading*, ASTM, West Conshohocken, PA, USA, 2012.

[18] J. K. Jeyapalan and B. A. Boldon, "Performance and selection of rigid and flexible pipes," *Journal of Transportation Engineering*, vol. 112, no. 5, pp. 507–524, 1986.

[19] MIDAS/GTS, *Analysis Reference*, MIDAS Information Technology Co., Ltd., Victoria, Australia, 2016.

[20] AWWA M45, *Fiberglass Pipe Design*, American Water Works Association, Denver, CO, USA, 2nd edition, 2005.